

DESIGN OF NEW SYNCHROTRON FOR HADRONTHERAPY

Akifumi ITANO, PhD.

Hyogo Ion Beam Medical Center

1-chome 2-1, Kouto, Shingu-cho, Ibo-gun, Hyogo, 679-5165, Japan

Abstract

A design of a synchrotron for hadrontherapy is presented. The synchrotron accelerates carbon beam up to 400 MeV/u and proton beam up to 230 MeV. It has super periodicity 2 and two long straight sections with FODOF structure and small dispersion, where multiturn injection and slow extraction devices are located. Control of chromaticity enables a superposition of the separatrices with different momentum and minimum losses would be obtained at the electrostatic septum.

INTRODUCTION

Recent successful operation of medical accelerators for hadrontherapy with carbon beam, HIMAC at National Institute of Radiological Sciences (NIRS) [1] and PATRO at Hyogo Ion Beam Medical Center (HIBMC) [2], accelerated the hadrontherapy projects in Europe [3-5]. The designed synchrotrons all have super periodicity 2 and a circumference 60 – 80 m. We design a new synchrotron with super periodicity 2 and two FODOF structure long straight sections. This structure produces a large phase advance in a transfer between an electrostatic septum and a following septum magnet, and was very successful at HIMAC and PATRO.

SPECIFICATIONS OF THE SYNCHROTRON

Table 1 summarizes the specifications of synchrotron. Figure 1 shows a layout of the synchrotron ring in a horizontal plane. It has a 10-fold FODO structure with super periodicity 2. Figure 2 shows betatron and dispersion functions at nominal tunes (Q_x, Q_y) = (2.35, 2.20). The ring has 2 long straight sections (FODOF) with small dispersion (< 0.3 m), which are used for a multiturn injection and a third order resonant slow extraction respectively. This small dispersion results a large dispersions (~ 7 m) at other sections. Horizontal aperture containing a corrected horizontal 3σ COD (± 4 mm) and momentum envelope with maximum $dp = \pm 0.7\%$ at rf capture is ± 102 mm in focusing quadrupole. This gives an enough space for injection and to have a 10 mm spiral step at extraction, where the momentum deviation would be reduced to $\pm 0.1\%$. Vertical aperture containing an uncorrected 3σ COD (± 12 mm) is ± 27 mm in defocusing quadrupole.

MULTITURN INJECTION

Four fast bump magnets are used to form a bump orbit. Entry point to the synchrotron of an injection electrostatic inflector (ESI) is 1.2 m upstream of a defocusing quadrupole in FODOF long straight sections. Septum of ESI is located at 44 mm from central orbit. Injection beam enters the ring at 47 mm from the central orbit and with an angle – 8.7mrad. The requested number of turns is 20. Emittances of injecting beam are assumed to be $\epsilon_x \pi = \epsilon_y \pi = 10 \pi$ mm·mrad.

Table1. Specifications of the Synchrotron

Particles	Proton and Carbon
Extraction Energy Range	100 -230MeV for p 100 -400MeV/u for Carbon
Beam Intensity (Circulating beam)	5×10^{10} ppp for p 4×10^9 ppp for Carbon
Maximum Dipole Field	1.433 T (rectangular type)
Tune (Q_x, Q_y)	(2.35, 2.20)
Injection Energy	5 MeV/u
Max. β_x / β_y	12.4 m / 23.1 m
Natural Chromaticity ξ_x / ξ_y	-1.063 / -2.238
Max. Dispersion D_x	7 m
Acceptance ($\epsilon_x \pi, \epsilon_y \pi$)	($200\pi, 10\pi$) in mm·mrad
Circumference	81.4 m
Super Periodicity	2
rf frequency	1.1 – 7.9 MHz (h=3)
Spill length	400ms
Maximum Repetition Rate	0.5 Hz for Carbon 1 Hz for proton
Extraction	3rd order resonance at 7/3

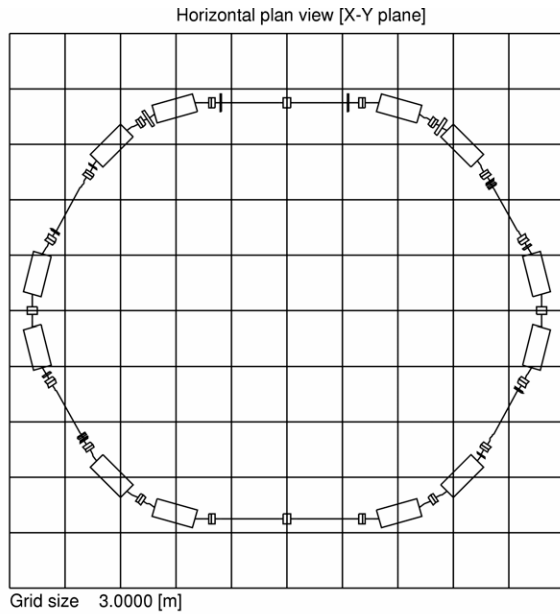


Fig.1 Layout of the synchrotron ring.

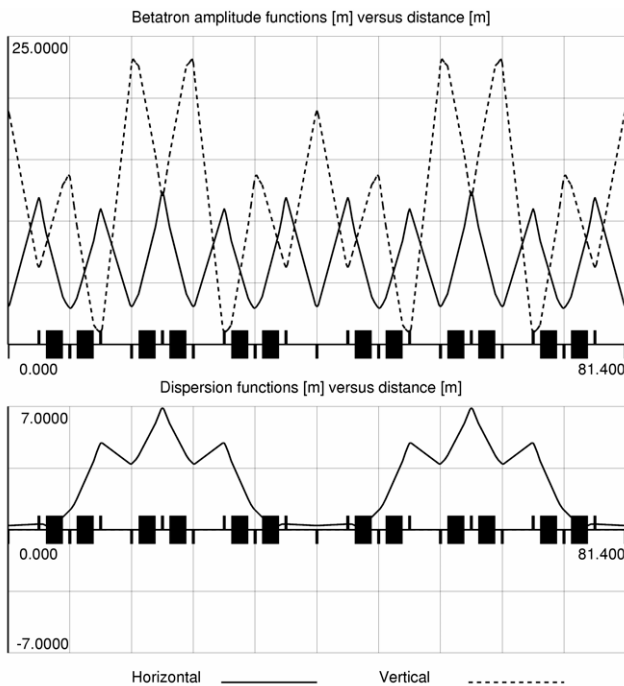


Fig.2 Betatron and Dispersion functions of the ring.

RF ACCELERATION

A single-gap rf acceleration cavity, composed of two quarter-wave ferrite-loaded coaxial lines excited in push-pull mode with figure-of-eight bias current loops, is located at downstream of ESI and defocusing quadrupole in FODOF section. As a dispersion function is small there, a beam phase and position monitor for rf frequency control will be located in other straight section, where dispersion is large. Required voltage is 5 kV (2.5 kV per half cavity). Aperture of the vacuum chamber is 200 mm in diameter. Outer, inner diameters and thickness of core

are 250, 160 and 25 respectively in mm. Assuming a maximum induction $B_{rf}=10\text{mT}\cdot\text{MHz}$ for Ni-Zn type ferrite, about 21 cores per half cavity are needed. Recent development of amorphous type magnetic alloy (such as FINEMET, VITROVAC6025F) gives a much larger value of rf magnetic field strength B_{rf} . Although this can decrease a number of cores required for the accelerating voltage, it also decreases a shunt impedance of a cavity and increases a required rf power. Anyway a large value of μQF -product $\sim 4 \times 10^9$ of amorphous alloy is interesting to obtain a large impedance together with its low bias current to control a permeability. With the amorphous alloy, the shunt impedance of the cavity is about 590Ω and the required amplifier power is 11 kW.

THIRD ORDER RESONANT SLOW EXTRACTION

Third order resonance at $Q_x=7/3$ is used for slow extraction. Two electrostatic deflectors ESD ($<80\text{kV/cm}$) are located in a first part of FODOF long straight sections. Two magnetic septa (0.5 and 1.5 T) are located in a second part. Two sextupoles located in diametrically opposite positions in the ring with inverse excitation are used for resonant excitation. This arrangement decouples a separatrix control from a chromaticity control. The sextupole with negative excitation is located at the position with a phase advance $p/3 \theta_n$ downstream of the first electrostatic septum of ESD.

$$p/3 \theta_n = p/3 \theta_0 + \pi/3 n = 5.69 \text{ rad with } n=5, p=7$$

$$p/3 \theta_0 = \varphi_{\text{esd}} - \pi/6$$

$$\varphi_{\text{esd}} = \arctan(\alpha x) = 0.975 \text{ rad}$$

$$\alpha x = 1.475 \text{ at ESD}$$

This locates the sextupoles near focusing quadrupoles and a large value of β_x ($\sim 11 \text{ m}$) permits a moderate sextupole strength 4 m^{-3} for resonance excitation at maximum energy.

Four slow bump magnets are used to form a 20-mm bump at ESD septum. Septum is located at 65 mm apart from a central orbit. Figure 3 shows a simulation of beam extraction. Initial ϵ_x is $20\pi \text{ mm}\cdot\text{mrad}$, which is a horizontal emittance at 400 MeV/u. Tunes are $(Q_x, Q_y) = (2.336, 2.20)$. Outward separatrix to the septum is nearly parallel to the x-axis in horizontal phase space. At the position of septum a spiral step is 10.2 mm and the beam angle is -6.0 mrad for $dp=0$. This angle can be controlled with an extra set of sextupoles.

HARDT CONDITION [6]

The beam contains particles with different amplitude, x and x' , in a phase space and a certain momentum spread dp . It can be represented as a series of ellipses (circles in a normalized phase space) for each dp . The circles become triangles by a resonance excitation. The size of a triangle corresponds to the last stable orbit. Any particles outside

the last stable triangle are lost along the outward separatrices, as is shown in Figure 3. Due to the chromaticity in the ring, the momentum spread will translate into a tune spread. Particles in the beam with different dp have the corresponding stable triangles in phase space with different sizes. Figure 4 shows three triangles and corresponding outward separatrices for $dp=0, \pm 0.1\%$ at the electrostatic septum. Chromaticities are set at their natural values. In the figure, an effect of $Dn dp/p$ is neglected because the dispersion vector is very small ($\sim 0.082 \text{ m}/2$). The separatrices are not superimposed and the particles move outward along different trajectories and reach the septum with different angles ($d\theta = \pm 0.7 \text{ mrad}$). This angular spread increases the effective thickness of the septum and so a beam loss. The angular spread will be eliminated if all the separatrices can be superimposed. This is achieved by the Hardt condition, which can be obtained by a removal of dp dependent terms from a general mathematical expression (with dispersion effect) of the separatrix. The Hardt condition is expressed with following expression:

$$D_n \cos(\pi - \delta\mu) + D'_n \sin(\pi - \delta\mu) = -4\pi/S \zeta_x.$$

$\delta\mu$: phase advance from resonance sextupole to ESD

S : normalized sextupole strength

D_n : normalized dispersion vector at ESD

ζ_x : horizontal chromaticity.

When the horizontal chromaticity is changed to -0.061 according to the condition, the three triangles in the figure become almost of equal sizes and the separatrices are superimposed on that of $dp=0$.

Figure 5 shows the last 3-turn trajectories in the ring for $dp=0, \pm 0.1\%$. Particle trajectories do not interfere with the septum of the injection electrostatic inflector (ESI) and is well inside the vacuum chambers.

Computer simulation was done with a code WinAGILE.

REFERENCES

- [1] E. Takada et al., Proc. of the 13th Sympo.on Accel. Sci. and Tech., Osaka, Japan (2001) pp.187-189.
- [2] A. Itano, Proc. of the 13th Sympo.on Accel. Sci. and Tech., Osaka, Japan(2001) pp.160-164.
- [3] U. Amalidi et al., The TERA project and the Centre for Oncological Hadrontherapy, INFN-LNF, Italy (1994).
- [4] J. Debus, Proposal for a dedicated ion beam facility for cancer therapy, DKFZ and GSI, Germany (1998).
- [5] Projet ETOILE, rapport LYCEN 2002-1 (A,B,C), Universite Claude Bernard Lyon 1, France (2002).
- [6] W. Hardt, Ultraslow extraction out of LEAR, CERN Internal Note PS/DL/LEAR Note 81-6 (1981).

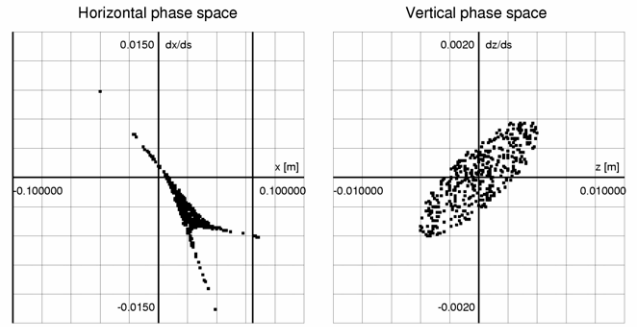


Fig.3 Phase space representation of the extraction.

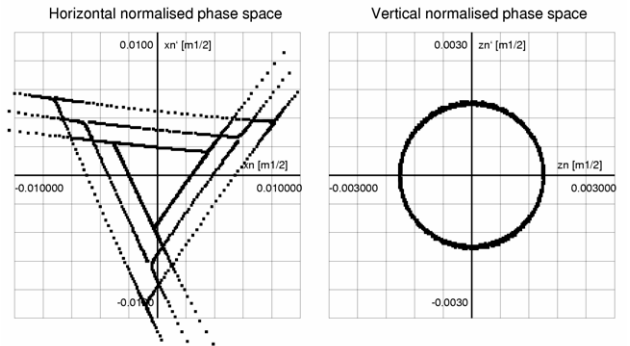


Fig. 4 Separatrices in the normalized phase space for $dp = -0.1\%$ (outer), 0% (middle) and 0.1% (inner).

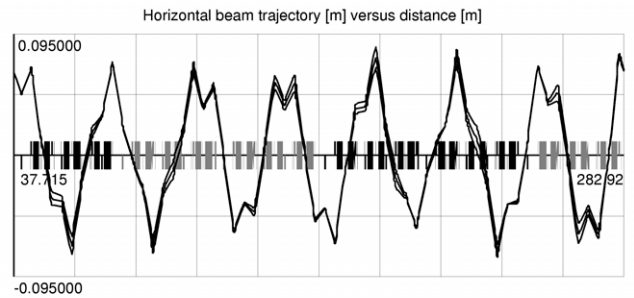


Fig. 5 Last 3-turn trajectories for $dp = 0, \pm 0.1\%$.